Profiling Atmospheric Water Vapor by Microwave Radiometry

J. R. WANG, J. L. KING,[1] T. T. WILHEIT AND G. SZEJWACH[2]

NASA/Goddard Space Flight Center, Greenbelt, MD 20771

L. H. GESELL, R. A. NIEMAN AND D. S. NIVER

Computer Sciences Corporation, Silver Spring, MD 20910

B. M. KRUPP

Systems and Applied Sciences Corporation, Riverdale, MD 20840

J. A. GAGLIANO

Georgia Institute of Technology, Atlanta 30332

(Manuscript received 9 September 1982, in final form 23 December 1982)

ABSTRACT

High-altitude microwave radiometric observations at frequencies near 92 and 183.3 GHz were used to study the potential of retrieving atmospheric water vapor profiles over both land and water. An algorithm based on an extended Kalman-Bucy filter was implemented and applied for the water vapor retrieval. The results show great promise in atmospheric water vapor profiling by microwave radiometry heretofore not attainable at lower frequencies.

1. Introduction

Water vapor is one of the most important constituents in the earth's atmosphere, as its spatial and temporal variations affect a wide spectrum of meteorological phenomena ranging from the formation of clouds to the development of severe storms. Its concentration, as measured in terms of relative humidity, determines the extinction coefficient of atmospheric aerosol particles and therefore visibility forecasts (Hanel, 1976). It provides an important input to tropical numerical weather prediction and energy budget studies, because the latent heat release due to condensation is crucial to the evolution of many tropical weather systems (Haydu and Krishnamurti, 1981). Its distribution over the surface of oceans can also be considered as a tracer of atmospheric motions (Prabhakara *et al.*, 1979). All these considerations point to the need for effective and frequent measurement of the distribution of atmospheric water vapor. Remote sensing by spaceborne infrared or microwave sensors (Hayden *et al.*, 1981; Prabhakara *et al.*, 1979, 1982; Staelin *et al.*, 1976; Grody *et al.*, 1980; Chang and Wilheit, 1979) is probably the most viable approach to the problem considering the vast expanse of the ocean areas. Past efforts in the microwave remote sensing of water vapor were generally limited to frequencies below 37 GHz (Staelin *et al.*, 1976; Grody *et al.*, 1980; Chang and Wilheit, 1979; Westwater and Guirand, 1980), although both theories and laboratory experiments (Waters, 1976 and references therein) have strongly suggested the prospect of using the absorption feature at 183.3 GHz (Shaerer and Wilheit, 1979; Rosenkranz *et al.*, 1982). The line strength at 22.2 GHz is weak, and in clear conditions, the atmosphere typically absorbs less than 20% of the radiation propagating through it at this frequency. Therefore, most of the attempts to retrieve water vapor by remote sensing near this frequency are necessarily limited to total integrated precipitable water (Staelin *et al.*, 1976; Grody *et al.*, 1980; Chang and Wilheit, 1979) and, in the downward-viewing geometry, to ocean areas where the low-emissivity water surface provides much-needed contrast. To retrieve water vapor in a few layers over oceans or land requires a strong absorption feature such as that around 183.3 GHz or a few infrared absorption bands (Hayden *et al.*, 1981). Profile retrievals discussed by Haydu and Krishnamurti (1981) generally require an *ad hoc* assumption about the functional dependence of the water vapor profile on either pressure or height.

[1] Deceased.

[2] NAS–NRC Resident Research Associate.

In the following, we explore the feasibility of profiling atmospheric water vapor with microwave radiometric measurements at frequencies near 92 and 183.3 GHz. The microwave radiometer used in the study is an airborne Advanced Microwave Moisture Sounder (AMMS) which has been developed in the past few years under a joint effort between NASA/Goddard Space Flight Center and Georgia Institute of Technology. A major difficulty in this development has been achieving adequate in-flight performance of the 183 GHz channels. During the CCOPE (Cooperative Convective Precipitation Experiment) flights in June 1981, the temperature sensitivity in the 183 GHz channels was adequate to permit a test of water vapor profile retrievals for the first time. An extended Kalman-Bucy filter technique (Ledsham and Staelin, 1978; Gelb, 1974) is employed here for water vapor retrieval from these data.

2. Theory

The theory of water vapor profiling using the 183 GHz water vapor line was initially discussed by Schaerer and Wilheit (1979). The present discussion derives largely from theirs. In a non-scattering medium, the application of the Rayleigh-Jean approximation reduces the equation of radiative transfer to a particularly simple form

$$\frac{dT_B}{dx} = \gamma(T_0 - T_B), \tag{1}$$

where T_B is the radiance expressed as a brightness temperature, T_0 is the thermometric temperature of the medium, and γ is the absorption coefficient of the medium. The derivative is along the direction of propagation. For nadir viewing this equation may be integrated to give the upwelling brightness:

$$T_{B\uparrow}(\infty) = \int_0^\infty e^{-\tau(h,\infty)}\gamma(\nu, h)T(h)dh + e^{-\tau(0,\infty)} \times \left[(1 - R)T_{\text{surf}} + R\int_0^\infty e^{-\tau(0,h)}T(h)\gamma(\nu, h)dh\right] + Re^{-2\tau(0,\infty)}T_{CB}, \tag{2}$$

where

$$\tau(z, y) = \int_z^y \gamma(\nu, x)dx$$

represents the optical depth between heights z and y, R is the reflectivity of the surface, $\gamma(\nu, h)$ the absorption coefficient of the atmosphere at a height h for a frequency ν, $T(h)$ the temperature profile of the atmosphere, T_{surf} the thermometric temperature of the surface, and T_{CB} the 2.7 K cosmic background temperature.

For temperature retrieval, the equation may be expressed in the form

$$T_{B\uparrow}(\infty) = \int_0^\infty J(\nu, h)T(h)dh + A, \tag{3}$$

where A represents the terms independent of the atmospheric temperature profile and $J(\nu, h)$, the temperature weighting function, is only weakly dependent on the temperature profile. These weighting functions form the basis of all schemes of retrieving temperature profiles from passive measurements.

Constituent retrievals, however, are inherently more difficult because the constituents enter into the brightness temperature equation through their contributions to γ, which appears both in the attenuation factor $\exp(-\int \gamma dx)$ and through the radiation factor $\gamma(\nu, h)T(h)$ so that the effect of γ at one location is dependent on γ at all other locations. Thus, one cannot express (2) in a form analogous to (3) for water vapor retrievals. It is, however, possible to express (2) in a variational form

$$\Delta T_{B\uparrow}(\infty) = \int_0^\infty G(h, \gamma(h), T(h))\Delta\gamma(h)dh, \tag{4}$$

where $\Delta T_{B\uparrow}$ is the infinitesimal brightness temperature change induced by the infinitesimal change $\Delta\gamma(h)$ in the absorption coefficient profile (caused by a change in the humidity profile). The function G then describes the water vapor information content of the brightness temperature at a given frequency. This variational weighting function depends very strongly on the temperature and humidity profiles as well as the viewing parameters (*e.g.*, frequency, polarization and viewing angle). Explicitly, this weighting function, in terms of relative humidity ρ/ρ_{sat} (1.00 = saturation), is given by

$$G(h, \gamma(h), T(h)) = \{e^{-\tau(h,\infty)}[T(h) - T_{B\uparrow}(h)] + Re^{-\tau(0,h)}e^{-\tau(0,\infty)}[T(h) - T_{B\downarrow}(h)]\}\frac{\partial\gamma(h)}{\partial\rho(h)}\rho_{\text{sat}}(h), \tag{5}$$

where $T_{B\uparrow}(h)$ and $T_{B\downarrow}(h)$ are the up- and down-welling brightness temperatures and $\rho_{\text{sat}}(h)$ is the saturation water vapor density at a height h. The partial derivative is generally well-approximated by

$$\frac{\partial\gamma(h)}{\partial\rho(h)} = \frac{\gamma(h)}{\rho(h)}. \tag{6}$$

Notice that there are two contributions to the weighting function given by Eq. (5), one proportional to $T(h) - T_{B\uparrow}(h)$ and the other to $T(h) - T_{B\downarrow}(h)$. Each is attenuated by the appropriate net opacity between h and the observer. If the surface has unit emissivity ($R = 0$) and a temperature of $T(0)$, then the weighting function vanishes identically at the surface. Since these assumptions are rather good for microwave frequencies > 100 GHz over land and for infrared frequencies over any background, the detectability of

near-surface water vapor will be poor under these conditions.

Fig. 1 shows these weighting functions for both land ($R = 0$) and water ($R = 0.3$) backgrounds for the three AMMS frequencies near 183 GHz as calculated for a midlatitude summer atmosphere (Air Force Cambridge Research Laboratory, 1965) with an assumed 100% relative humidity. Fig. 2 shows the same calculations for 10% relative humidity; note the scale change from Fig. 1. The gross change of these weighting functions emphasizes the nonlinear nature of the water vapor profile retrieval problem.

3. The retrieval algorithm

An early attempt to retrieve water vapor profiles using the absorption feature near $\nu = 183$ GHz was given by Schaerer and Wilheit (1979). It was shown by these authors that, at least theoretically, microwave radiometry around this absorption line could yield a fair estimate of water vapor profiles over ocean even with a crude algorithm. In the following discussion we will apply the Kalman-Bucy filter technique (Gelb, 1974) as was explored by Ledsham and Staelin (1978) for atmospheric temperature profile retrieval. To obtain water vapor profiles, the retrieval algorithm has to be modified to account for the change of the weighting functions due to temporal and spatial variations of the water vapor itself. The theory of the Kalman-Bucy filter has been widely discussed (Gelb, 1974; Ledsham and Staelin, 1978),

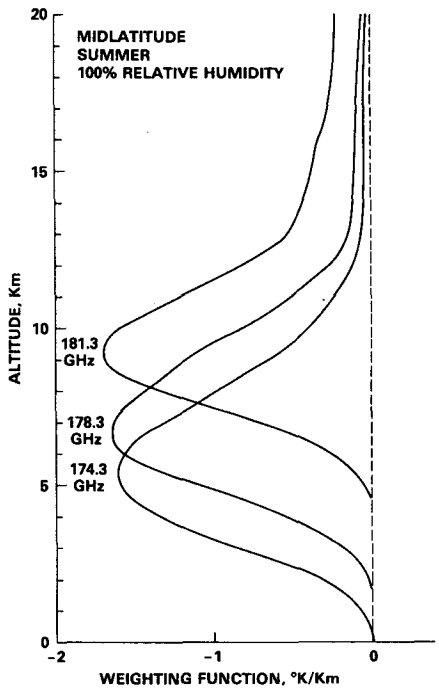

FIG. 1. Relative humidity weighting functions for a midlatitude summer atmosphere over land and ocean.

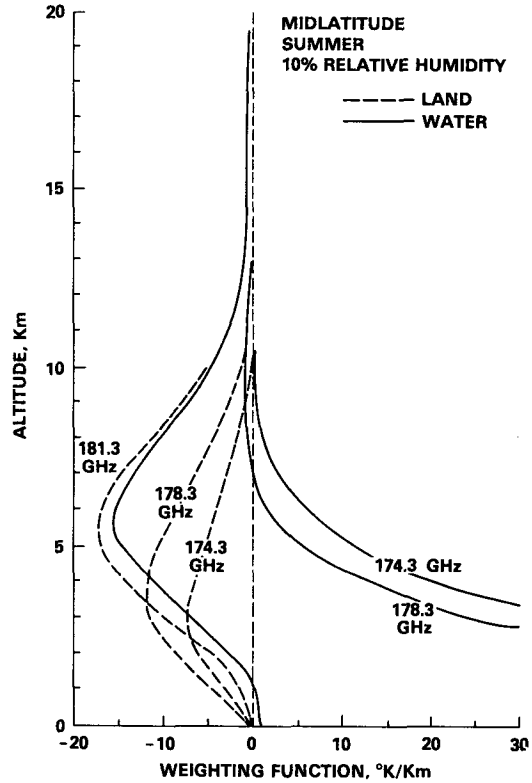

FIG. 2. Relative humidity weighting functions for a midlatitude atmosphere over land and ocean.

and thus only a few equations relevant to the present discussion will be quoted in the following. If the process to be estimated is represented by an n vector $\mathbf{X}$ (*e.g.*, relative humidities at different altitudes), and the observed process, by an m vector $\mathbf{Z}_i$ (*e.g.*, T_B's), then

$$\mathbf{Z} = f(\mathbf{X}) + \mathbf{N}. \tag{7}$$

This is essentially the radiative transfer equation for T_B's [Eq. (2)] with additional instrument noise represented by an m vector $\mathbf{N}$. $\mathbf{N}$ can be taken as a zero mean white Gaussian process with covariance matrix $\mathbf{Q}$. Expanding $f(\mathbf{X})$ around the *a priori* conditional mean $\mathbf{X}(-)$, and retaining only the constant and the linear terms, the final expression for the optimum estimate of $\mathbf{X}$ using a simple Bayesian approach is (Ledsham and Staelin, 1978)

$$\hat{\mathbf{X}}(+) = \hat{\mathbf{X}}(-) + \mathbf{K}[\mathbf{Z} - f(\mathbf{X}(-))], \tag{8}$$

with

$$\mathbf{K} = \mathbf{P}(-)\mathbf{H}^T(\hat{\mathbf{X}}(-))[\mathbf{H}(\hat{\mathbf{X}}(-)) \times \mathbf{P}(-)\mathbf{H}^T(\hat{\mathbf{X}}(-)) + \mathbf{Q}]^{-1}, \tag{9}$$

$$\mathbf{P}(+) = [\mathbf{I} - \mathbf{K}\mathbf{H}(\hat{\mathbf{X}}(-))]\mathbf{P}(-), \tag{10}$$

$$\mathbf{H}(\hat{\mathbf{X}}(-)) = \left.\frac{\partial f(\mathbf{X})}{\partial \mathbf{X}}\right|_{\mathbf{X}=\mathbf{X}(-)}. \tag{11}$$

Here the minus or plus sign in parentheses refers to the quantity before or after a given iteration of the solution. The optimum estimate of a quantity is denoted by a caret. **I** is the n by n identity matrix, **H** is an m by n matrix representation of the relative humidity weighting functions ($\mathbf{H}^T$ is the transpose of **H**), and **K** is the Kalman gain. $\mathbf{P}(-)$ is the n by n error covariance matrix associated with $\mathbf{X}(-)$. **Q** is assumed to be a diagonal matrix with each diagonal element being the variance of the noise (taken to be 0.5 K after averages over 150 samples) in the corresponding AMMS channel. The weighting functions **H** and $\mathbf{P}(-)$ are updated in each iteration process.

The relative humidity is extrapolated from its value at the top reference level to zero at the altitude of 17 km. Three levels at 2.30, 4.20 and 5.84 km altitudes are selected for water vapor retrieval. The relative humidities at other altitudes are extrapolated or interpolated from the retrieved values at these three altitudes and used in the next iteration process. $\mathbf{P}(-)$ is then (in units of relative humidity squared) chosen to be

$$\mathbf{P}(-) = \begin{pmatrix} 20 & 10.63 & 6.17 \\ 10.63 & 20 & 11.60 \\ 6.17 & 11.60 & 20 \end{pmatrix}, \qquad (12)$$

when the relative humidity is expressed in percent. This agrees qualitatively with the autocorrelation matrix of the humidity profiles observed over the North Atlantic (Dombkovskaya, 1971). It is found that $\mathbf{P}(+)$ is generally smaller than $\mathbf{P}(-)$ after application of Eq. (10). Therefore, each element of $\mathbf{P}(+)$ is increased by 10% of its original value after each iteration in order to keep $\mathbf{P}(-)$ in a reasonable range and to help stabilize the retrieval process. To make sure that $\mathbf{P}(+)$ stays positive semi-definite at each step of the retrieval, the "square-root algorithm" (Kaminiski *et al.*, 1971) is also used in the implementation of the Kalman-Bucy filter.

4. Instrument

The Advanced Microwave Moisture Sounder (AMMS) is a 4-channel, mechanically scanned imaging microwave radiometer. The major elements of AMMS are depicted as a block diagram in Fig. 3. The 92 GHz channel is a conventional superheterodyne receiver wherein the incoming signal is beat with a local oscillator signal (92 GHz) and the resulting signal is amplified by the intermediate frequency (IF) amplifier which is sensitive to a band from 1 to 2 GHz. The channel is therefore sensitive to two bands, 90–91 and 93–94 GHz. Since there is a rather broad window in the atmospheric absorption spectrum between the oxygen features near 60 and 118 GHz, the large range of frequencies associated with this channel produces no problem in interpretation. The 183 GHz channel employs a novel second harmonic mixer which doubles the local oscillator frequency internally. The signal from this mixer is separated into three bands using a triplexer and then amplified by three IF amplifiers centered at 2, 5 and 9 GHz; the bandwidth of each is ~20% of its center frequency. The local oscillator is tuned to 91.65 GHz so that the pairs of received bands are centered on 183.3 GHz, the center of the water vapor resonance. The near symmetry of this line then makes the two bands received by each channel equivalent. These channels are referred to as 183 ± 2, 183 ± 5 and 183 ± 9 GHz.

Another novel feature of AMMS is the super chopper, which consists of a rapidly rotating toothed aluminum wheel. When a tooth is in front of the feed

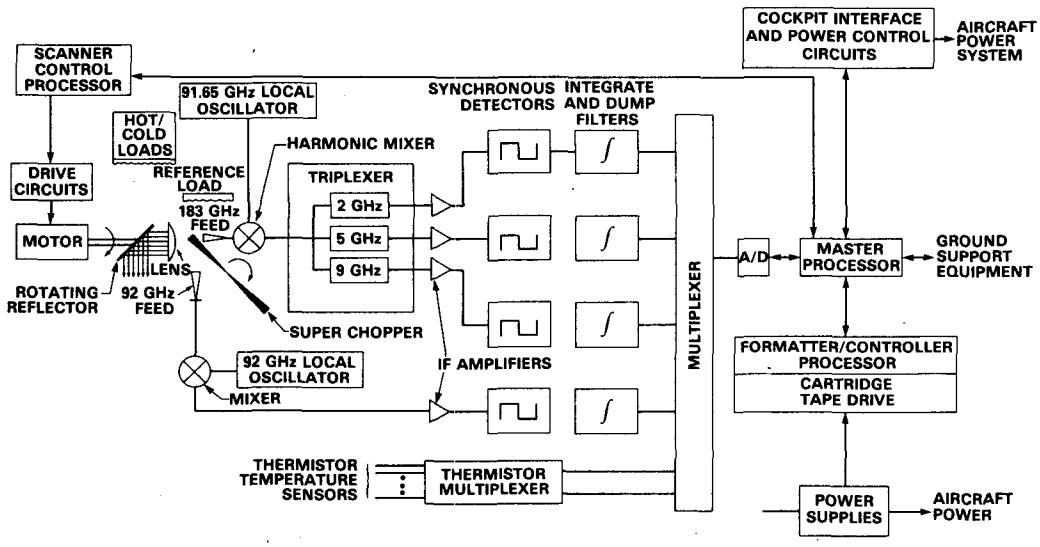

FIG. 3. Block diagram of the Advanced Microwave Moisture Sounder (AMMS).

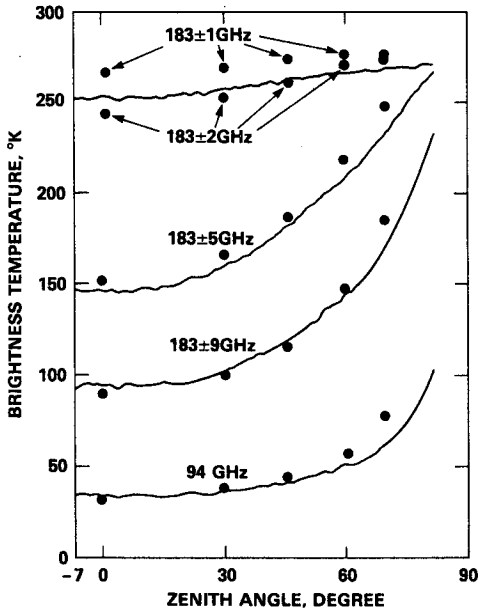

FIG. 4. The zenith angle dependence of downwelling brightness temperatures as observed by AMMS on 4 February 1980 at Georgia Institute of Technology, Atlanta.

horns, the 92 GHz feed views the earth scene or a calibration load through the lens and the rotating reflector, while the 183 GHz feed views the reference load by reflection off the tooth. When a gap is in front of the feeds, the 92 GHz feed views the reference load, and the 183 GHz feed, the Earth scene. Thus, the super chopper provides both the modulation which is required in a Dicke radiometer and also duplexes the incoming signal between the two feeds.

The lens and reflector represent a 15 cm aperture which gives an angular resolution of 2° at 92 GHz and 1° at 183 GHz. The beam is scanned in 50 steps of 1.8° from 45° to the left, through nadir, to 45° to the right with total scanning and retrace time of 3.3 s. After every six scans, the reflector reflects the signal from a heated (60°C) calibration load and from a cooled (−20°C) calibration load for 10 samples, resulting in a total frame time of 23 s. Every tenth frame is modified to view the Earth at nadir for 150 sample periods (equivalent to three scans) and at 45° to the right for 150 sample periods *in lieu* of the ±45° scanning. It is these so-called "stare mode" data that are used in the water vapor retrievals discussed in the next sections. A more detailed description of the engineering design and operation of the instrument is given by Gagliano and McCheehy (1981).

The in-flight calibration of AMMS was made by banking the aircraft to a 60° roll angle so that the sensor viewed the cold sky 15° above the horizon at an altitude of 15 km. On 4 February 1980, the AMMS was also tested by scanning the sky above the campus

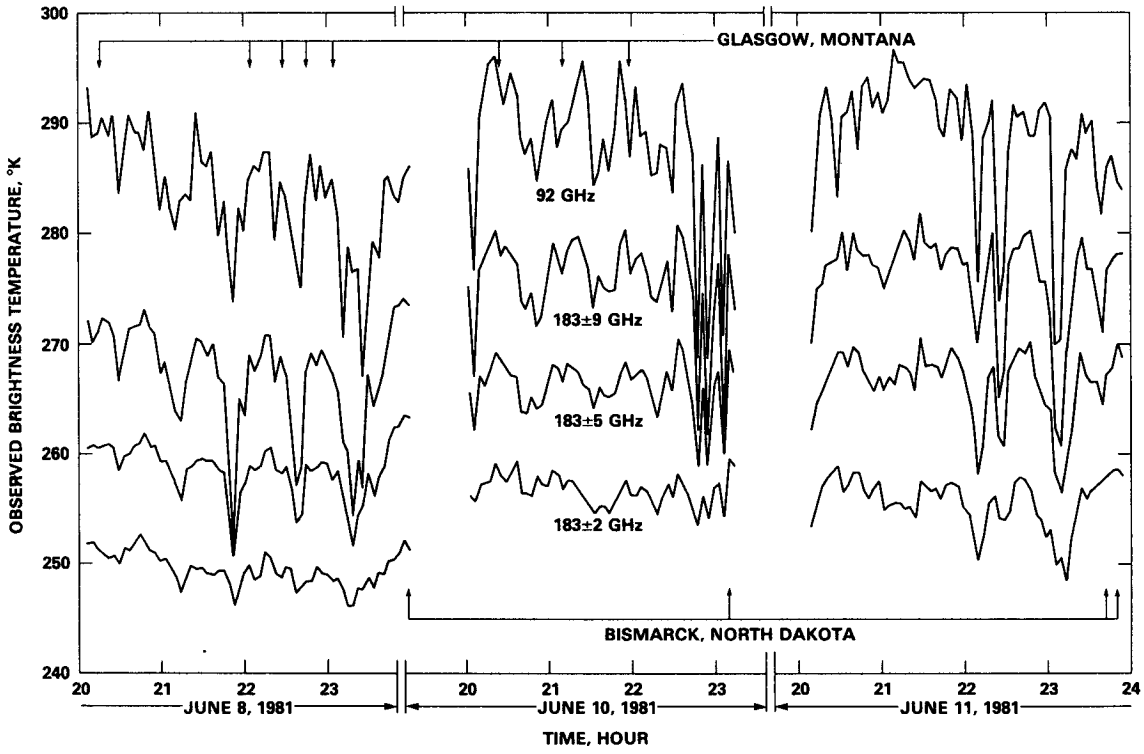

FIG. 5. The time history of the upwelling brightness temperature observed by airborne AMMS on 8, 10 and 11 June. The observations were made at nadir-viewing geometry with an aircraft speed of ~750 km h^{-1}.

of Georgia Institute of Technology, over zenith angles from near the horizon (83°) through zenith and beyond (7°). The day was clear and cold, and the measurement was made around 2200 GMT. The results of the measurements are shown in Fig. 4 where the brightness temperatures T_B were plotted as a function of zenith scan angle for each of four frequency channels. The solid curves give the results of the measurements and the solid circles show the results of radiative transfer calculations based on the nearest radiosonde (Athens, GA), some 80 km away from the test site.

Clearly, the measured and the calculated T_B's agreed quite well over a wide range of zenith angles, 0–60°. Calculations were performed at frequencies of 182.3 and 181.3 GHz to show how sensitive the radiometer is to small frequency changes near the peak of water vapor absorption. As indicated in the figure, the calculated T_B differed by 20 K when the frequency was changed by only 1 GHz.

5. The experiment

During May–June 1981, nine flights of the NASA WB-57F aircraft were made over portions of Montana and North Dakota as part of CCOPE (Knight, 1982). AMMS was one of many sensors included in the mission. Although the main objective of CCOPE was to study storm-related phenomena, the flights of 8, 10 and 11 June were relatively free from storm systems. Fig. 5 shows the variations of T_B with time observed at nadir in "stare mode" from all three flights. The arrows in the figure indicate the times when the aircraft locations were closest to the two radiosonde stations: Bismarck, North Dakota; and Glasgow, Montana. The observed T_B's at these times are listed in Table 1 for comparison with those calculated from Eq. (2). The T_B calculations were made with the 0000 GMT radiosonde data of 9, 11, 12 June and with $R = 0.02$ and $R = 0.1$ (a fairly realistic range over land at frequencies near 90 GHz). Notice that for the two channels nearest 183.3 GHz, the calculated T_B's changed by only 0.2 K or less when R was varied from 0.02 to 0.1, because the atmosphere was essentially opaque to the ground radiation at these frequencies. The corresponding change at 92 GHz ranged from 14 to 16 K.

A comparison of the observed and calculated T_B's in Table 1 reveals differences up to 9 K in some cases. Contributions from one or more of the following factors could be the cause of these differences. First, there is always some uncertainty about the absolute calibration accuracy of AMMS. Uncertainty of this nature is estimated to be no more than 3 K. A 9 K bias

TABLE 1. The observed and calculated brightness temperatures.

Location	Data type	Date June	Time (GMT)	Brightness temperature (K) 183 ± 2 GHz	183 ± 5 GHz	183 ± 9 GHz	92 GHz	Remarks
Glasgow, MT	Observed	8	2016	251.0	260.6	271.5	289.7	
		8	2205	249.1	258.7	268.2	285.5	
		8	2228	249.2	258.4	268.0	283.9	
		8	2246	248.4	258.6	268.1	284.9	
		8	2305	248.5	257.4	266.4	283.2	
		10	2025	258.1	268.5	279.0	293.8	
			2111	257.9	267.5	278.0	289.7	
			2159	256.7	267.7	278.1	290.7	
	Calculated	8	2300	251.5	267.2	276.7	286.4	
		10	2300	259.1	270.8	278.8	286.5	$R = 0.02$
		8	2300	251.5	267.1	275.1	270.9	
		10	2300	259.1.	270.6	276.7	270.8	$R = 0.1$
Bismarck, ND	Observed	8	2359	251.3	263.3	273.5	286.1	
		10	2310	259.5	269.5	278.2	286.6	
		11	2342	258.0	267.2	276.7	286.0	
		11	2350*	257.5	267.5	273.7	207.6	
	Calculated	8	2300	255.2	268.1	277.5	290.6	
		10	2300	255.4	266.7	275.6	286.3	
		11	2300	255.1	267.2	275.8	286.3	$R = 0.02$
		8	2300	255.2	268.1	276.8	276.6	
		10	2300	255.4	266.7	274.8	272.3	
		11	2300	255.1	267.2	275.1	272.4	$R = 0.1$
		11	2300	255.1	267.0	270.6	213.0	$R = 0.4$

* Observation over Lake Sakakawea near Bismarck.

in the absolute calibration is rather unlikely. Second, some contributions may come from the propagation of error in the calculated T_B's due to the uncertainties in the absorption coefficients γ and the radiosonde measurements. For example, when γ, as given by Waters (1976), is changed by ±20% in absolute magnitude, the corresponding changes in the calculated T_B's are ±1.6 K at the three high-frequency channels and ±1.0 K at 92 GHz when using the 0000 GMT 11 June Bismarck radiosonde measurement of temperature, pressure and humidity profiles. Third, if there are clouds in the field of view of AMMS, significant errors could result. This could be the case for the flight near Glasgow on 8 June. From the visible photographs taken during the flight, cloud cover is evident during each overpass of the Glasgow region. Figs. 6a and 6b show three sets of relative humidity and temperature profiles observed at 12 h intervals, from 1200 GMT 8 June to 1200 GMT 9 June. The high relative humidity at 7–9 km around 2300 GMT probably indicates the height of the cloud cover. Normally, the relative humidity within the cloud is expected to be much higher than the 70% indicated in the figure. Also, Glasgow is some 120 km away from the direct underpass of the aircraft flight; certainly this is a possible source of the error. A relative humidity of 95% or more at 7–9 km would lower the calculated T_B's and make them more comparable to those observed by AMMS.

Figs. 6a and 6b also show a substantial change in relative humidity profiles in 12 h. This implies that radiosonde observations actually coincident in time and location with an AMMS overflight are required in order to adequately assess the system's performance. Data sets associated with flights over Bismarck on 8, 10 and 11 June more or less satisfy these requirements. Aerial photographs taken on 8 June indicate a slight cloud cover over the Bismarck area. Therefore, the data set obtained on 10 and 11 June were used for testing the retrieval algorithm as discussed in the next section.

6. Results

The results of atmospheric water vapor retrieval using the T_B's observed by AMMS on 10 and 11 June near Bismarck are shown in Figs. 7, 8 and 9. Figs. 7 and 8 show the humidity profiles derived from the retrieval over land along with the radiosonde observations for each day. The retrieved profiles in Fig. 9 are based on the AMMS data obtained on 11 June over nearby Lake Sakakawea. The initial relative humidity profile in each retrieval is assumed to be uniform at 50% below 5.84 km and then linearly decreased to zero at 17 km. The temperature profiles used in the retrieval are obtained from Bismarck radiosonde observations around 0000 GMT on 11 and 12 June. Retrievals over water using all four channels and also using only the three channels near 183 GHz were made to test the usefulness of the window channel at 92 GHz. Surface temperatures were not measured by this instrument. Therefore, two different sur-

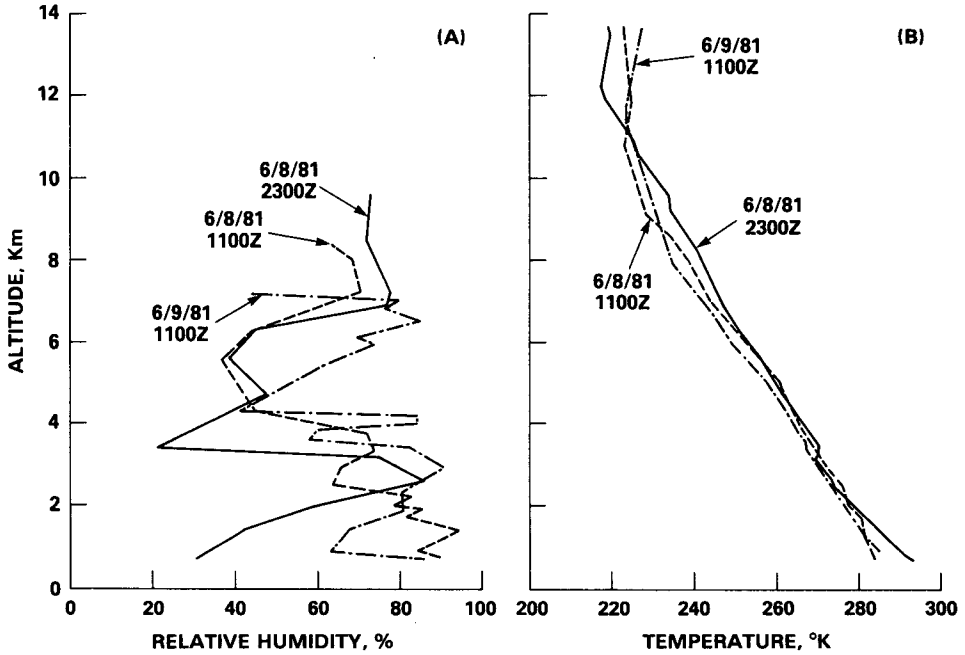

FIG. 6. Three consecutive radiosonde observations of (a) relative humidity and (b) temperature profiles at Glasgow, Montana.

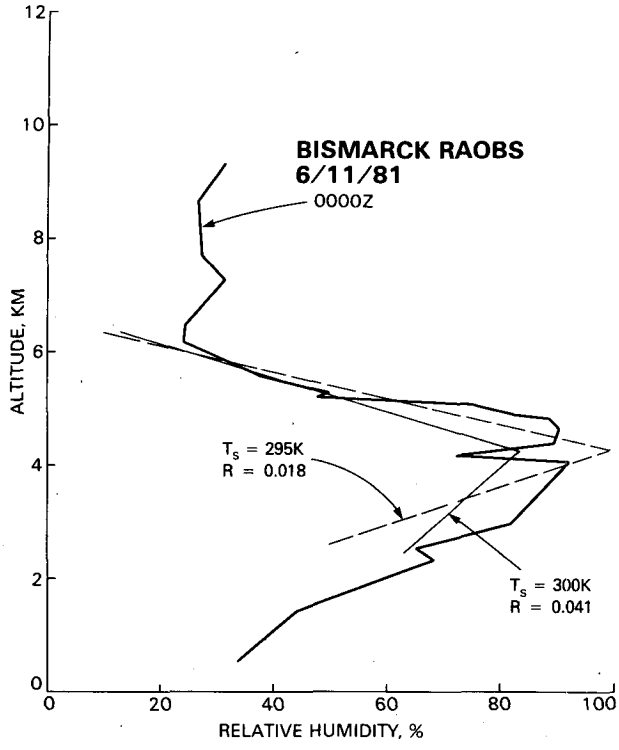

FIG. 7. Relative humidity retrieval with data obtained by AMMS over land near Bismarck, North Dakota, 11 June 1981.

face temperatures, 295 and 300 K for land and 285 and 295 K for water, comparable to the lowest level air temperature of 293 K observed by radiosonde, are separately used in the retrieval. The reflectivity over land is derived by applying Eq. (2) to the 92 GHz measurement at each iteration, and that over water is determined by its temperature and frequency dependence based on data compiled by Nieman (1979). Approximately 30 iterations are required to arrive at each of the final stable humidity profiles shown in the figures.

The retrieved humidity profiles over land in the altitude range of 4–7 km shown in Figs. 7 and 8 agree well with those of the radiosonde observations. On the other hand, the retrieved relative humidities below 4 km are strongly affected by surface temperature. A change of 5 K in surface temperature could result in as much as 30% difference in the retrieved relative humidities. This suggests the need of an accurate simultaneous surface temperature measurement over land.

The two relative humidity profiles resulting from the 3-frequency retrievals at lake surface temperatures of 285 and 295 K are quite comparable, suggesting that the retrieval is not very sensitive to water temperature. However, there is a substantial difference in the final humidity profiles obtained from the 3-frequency and the 4-frequency retrievals. While the two profiles from the 3-frequency retrieval agree well with that of the radiosonde observation, the one from the 4-frequency retrieval is ~20% smaller in the altitude range of 2–5 km. This is not a surprising result considering the 6 K difference between the calculated and the observed 92 GHz brightness temperatures over water listed in Table 1. If we assume that there is no significant error in the instrument calibration and reduce the atmospheric absorption coefficient at 92 GHz by 30%, then the difference between the 3-frequency and the 4-frequency retrieved humidity profiles becomes negligible. The usefulness of the 92 GHz channel to the retrieval is not clear in this case.

We note that in Figs. 7–9, the relative humidities are retrieved at three fixed reference altitudes. It can be shown that the selection of these altitudes is not critical. Retrievals for different reference altitudes in the 1–7 km region results in relative humidities not very different from the linearly interpolated values given in the figures. Selection of reference altitudes above 7 km does not give a good retrieval because of the limited AMMS frequency channels. Perhaps additional frequency channels closer to 183.3 GHz absorption peak, *e.g.*, 183.3 ± 0.5 GHz and 183.3 ± 1 GHz, are needed to improve water vapor retrieval at high altitudes. We also point out that the relative humidity profiles observed by radiosonde during these two time periods happen to be very similar. More studies with different humidity profiles are re-

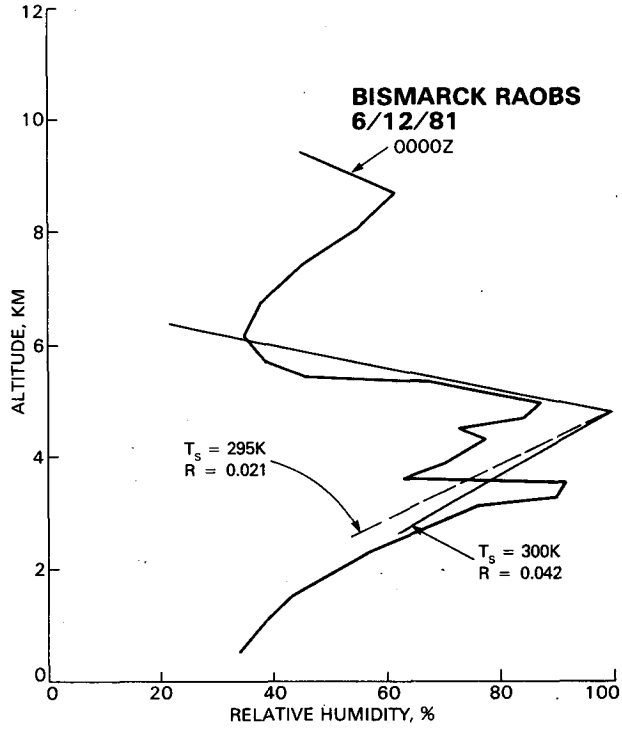

FIG. 8. As in Fig. 7, but for 12 June 1981.

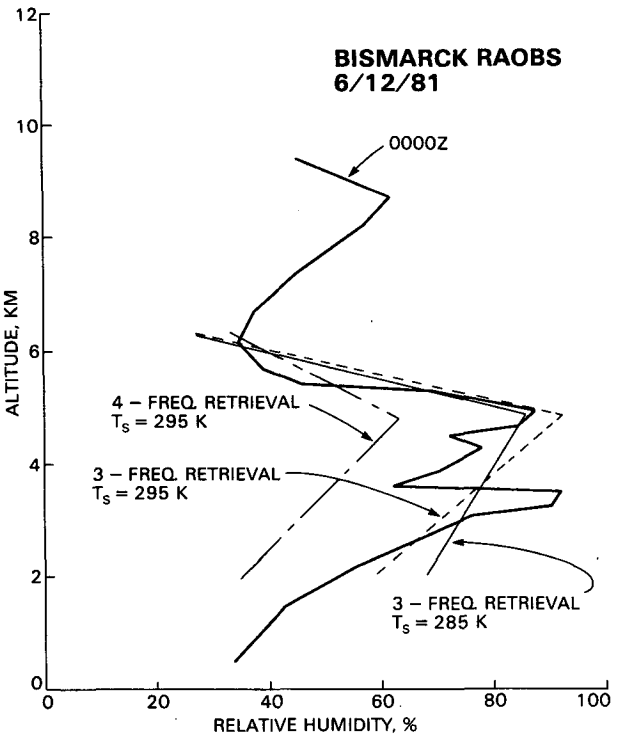

FIG. 9. As in Fig. 8, but for data over Lake Sakakawea near Bismarck, North Dakota.

quired to test the validity of the retrieval technique fully.

7. Conclusions

An Airborne Advanced Microwave Moisture Sounder (AMMS) was assembled and tested for profiling the atmospheric water vapor. Radiosonde data from two weather stations near the aircraft flight paths were used both to simulate the radiometric response of AMMS frequency channels and to study the retrievability of water vapor profiles. The results presented in the last section show a good potential for profiling atmospheric water vapor with microwave radiometry around the strong water vapor absorption line at 183.3 GHz. There is also an indication that retrieving water vapor over land in the altitude range of 1–3 km may be possible if a precision measurement of surface temperature is available. This is not expected from the theoretical discussion given in Section 2. Zeng (1979) had also pointed out the difficulty in boundary-layer water vapor retrieval over land using either an infrared or microwave approach. More case studies are required to see if the low-altitude water vapor is really retrievable over land, particularly below 4 km.

The AMMS instrument has a temperature sensitivity of ~3 K at the three frequency channels near 183.3 GHz and a sensitivity of ~1.5 K at 92 GHz. To improve the precision of the measurements, 150 samples of brightness temperatures measured in each of four channels are averaged and their mean values used to arrive at the retrieved relative humidities in Figs. 7–9. In remote sensing application a temperature sensitivity of about 1 K is desired. With present technology in microwave radiometry, such a temperature sensitivity is not difficult to achieve.

To profile the atmospheric water vapor by microwave radiometry requires a reliable atmospheric temperature profile as input in the retrieval algorithm. The error in the measurement of the temperature profile certainly will have a significant impact on the water vapor retrieval accuracy. To see qualitatively the effect of the temperature uncertainty on the retrieved relative humidity, retrievals were performed for the AMMS data obtained near Bismarck on 11 June over land with the radiosonde observed atmospheric temperature values shifted by a certain amount at all altitudes. The results were then compared with the retrieved profiles shown in Fig. 8. It was found that a 1 K shift in the temperature profile changed the retrieved relative humidity by less than 10% at any reference level. A temperature shift of 4 K produced variations in the retrieved relative humidity values exceeding 50%. Thus, a precision temperature measurement is needed in order to obtain an adequate estimate of the atmospheric water vapor profile.

The water vapor retrieval accuracy also depends on the reliability of the absorption coefficient γ. As an example, when the values of γ (Waters, 1976) are multiplied by a factor of 0.8 and then used in the retrieval of relative humidity with the measured T_B's on 10 June near Bismarck, the retrieved values of relative humidity in the 2–7 km altitude range increase by 6–9% over the ones shown in Fig. 7. This clearly indicates the need for precise information on γ.

Finally, the effect of cloud cover on a water vapor retrieval needs to be fully investigated. This effect has been brought up previously (Schaerer and Wilheit, 1979) but a systematic study has never been conducted to determine its impact on the retrieval accuracy. From a limited CCOPE observation, the presence of a cloud cover causes a decrease in brightness temperature in each AMMS channel. A preliminary investigation of the effect of a cloud cover on humidity retrieval shows that a retrieval without providing for the existence of atmospheric liquid water generally results in an overestimate of the atmospheric water vapor immediately above and below the cloud cover. Further experiments with a sensor like AMMS over both land and ocean and with simultaneous radiosonde observations should be performed more extensively in the future to study the effect of cloud cover and assess the prospect of retrieving the atmospheric water vapor profile with a microwave radiometer.

REFERENCES

Chang, A. T. C., and T. T. Wilheit, 1979: Remote sensing of atmospheric water vapor, liquid water, and wind speed at the ocean surface by passive microwave techniques from Nimbus-5 satellites. *Radio Sci.*, **14,** 793–802.

Dombkovskaya, E. P., 1971: Some characteristics of the vertical structure of the humidity field over the North Atlantic. *Advances in Satellite Meteorology,* A. I. Burtsev, P. N. Belov and S. A. Musaelyan, Eds., Wiley, 256–264.

Gagliano, J. A., and J. J. McCheehy, 1981: Advanced microwave moisture sounder (AMMS) for WB-57F CCOPE mission. Technical report for Project A-2904, Georgia Institute of Technology, 40 pp.

Gelb, A., Ed., 1974: *Applied Optimal Estimation.* The MIT Press, 374 pp.

Grody, N. C., A. Gruber and W. C. Shon, 1980: Atmospheric water content over the tropical Pacific derived from the Nimbus-6 Scanning Microwave Radiometer. *J. Appl. Meteor.*, **19,** 986–996.

Hanel, G., 1976: The properties of atmospheric aerosol particles as functions of the relative humidity at thermodynamic equilibrium with the surrounding moist air. *Advances in Geophysics,* Vol. 19, Academic Press, 73–188.

Hayden, C. M., W. L. Smith and H. M. Wolf, 1981: Determination of moisture from NOAA polar orbiting satellite sounding radiances. *J. Appl. Meteor.*, **20,** 450–466.

Haydu, K. J., and T. N. Krishnamurti, 1981: Moisture analysis from radiosonde and microwave spectrometer data. *J. Appl. Meteor.*, **20,** 1177–1191.

Kaminski, P. G., A. E. Bryson, and S. F. Schmidt, 1971: Discrete square root filtering: a survey of current techniques, *IEEE Trans. Auto. Control,* **AC-16,** 727–736.

Knight, C. A., Ed., 1982: The Cooperative Convective Precipitation Experiment (CCOPE), May 18–August 7, 1981. *Bull. Amer. Meteor. Soc.*, **63,** 386–398.

Ledsham, W. H., and D. H. Staelin, 1978: An extended Kalman-Bucy filter for atmospheric temperature profile retrieval with a passive microwave sounder. *J. Appl. Meteor.*, **17,** 1023–1033.

Nieman, R. A., 1979: Airborne passive microwave observations of raindrops and ice particles during tropical storm Cora. Computer Sciences Corp., CSC/TM-79/6175, Silver Spring, MD, 67 pp.

Prabhakara, C., G. Dalu, R. C. Lo and N. R. Nath, 1979: Remote sensing of seasonal distribution of precipitable water vapor over the oceans and the interface of boundary-layer structure. *Mon. Wea. Rev.*, **107,** 1388–1401.

Rosenkranz, P. W., M. J. Komichak and D. H. Staelin, 1982: A method for estimation of atmospheric water vapor profiles by microwave radiometry. *J. Appl. Meteor.*, **21,** 1364–1370.

Schaerer, G., and T. T. Wilheit, 1979: A passive microwave technique for profiling of atmospheric water vapor. *Radio Sci.*, **14,** 371–375.

Staelin, D. H., K. F. Kunzi, R. L. Pettyjohn, R. K. L. Poon, R. W. Wilcox, and J. W. Waters, 1976: Remote sensing of atmospheric water vapor and liquid water with the Nimbus-5 microwave spectrometer. *J. Appl. Meteor.*, **15,** 1204–1214.

Waters, J. W., 1976: Absorption and emission by atmospheric gases. *Methods of Experimental Physics,* Vol. 12, Part B, Academic Press, 142–176.

Westwater, E. R., 1978: The accuracy of water vapor and cloud liquid determined by dual-frequency ground-based microwave radiometry. *Radio Sci.*, **13,** 677–685.

Wilheit, T. T., A. T. C. Chang, J. L. King, E. B. Rodgers, R. A. Nieman, B. M. Krupp, A. S. Milman, J. S. Stratigos and H. Siddalingaiah, 1982: Microwave radiometric observations near 19.35, 92 and 183 GHz of precipitation in Tropical Storm Cora. *J. Appl. Meteor.*, **21,** 1137–1145.

Zeng, Q., 1979: Theoretical problems of infrared remote sensing of the atmosphere. *Sci. Sinica,* **22,** 555–564.